

Several inter-related factors lead to complicated heterogeneities in sedimentary rocks, including the depositional settings, diagenetic processes, as well as tectonics and burial/thermal evolution of the basin (Cantrell et al. 2001; Roure et al. 2005; Ehrenberg et al. 2007; Rahimpour-Bonab et al. 2010). Substantial heterogeneities are often associated with carbonate reservoir rocks, resulting in a significant challenge for the optimization of hydrocarbon production and recovery (Ahr 2008), underground storage of gas (e.g. carbon capture and storage—CCS), freshwater and geothermal energy applications. In order to characterize properly such heterogeneities, studies of diagenetic phases (products) have to be combined to classical sedimentological investigations and basin analyses (e.g. burial history).

By ‘characterization’, description and classification are invoked. The diagenetic phases, which are produced by certain processes under specific conditions, are precisely described and then ascribed to carbonate diagenetic realms (see above, Chap. 1). Accordingly, predictive deductions could be applied concerning the extent of such phases and their impacts on the host-rocks at various scales. Diagenetic phases cover a wide range of types, some of which are: (i) mineralogical phases, such as cements; (ii) fluid phases, such as trapped fluid inclusions; (iii) transformed matter, such as dissolved material; and (iv) and resulted pore space. They are commonly investigated with a variety of tools, somehow specific to the type of phases at

hand, which make the state of the art of today’s characterization workflows for diagenesis.

2.1 State of the Art (Characterization of Diagenesis)

Classical carbonate diagenesis studies make use of a wide range of analytical techniques and aim to describe and explain specific, relatively time-framed, diagenetic processes (e.g. Nader et al. 2004; Gasparrini et al. 2006; Fontana et al. 2010; Ronchi et al. 2011; Swennen et al. 2012). Currently used techniques combine petrographic (conventional, cathodoluminescence, fluorescence, scanning electron microscopy with energy dispersive spectrometer—SEM/EDS, and 3D X-ray micro-computed tomography, micro-CT), geochemical (major/trace elements, stable oxygen and carbon isotopes, strontium isotopes, magnesium isotopes, clumped isotopes), and fluid inclusion analyses (microthermometry, Raman spectrometry, crush-leach analysis), providing the state of the art characterization tools and further independent arguments to support or discard any of the proposed conceptual models.

Diagenetic studies usually follow classical sedimentological descriptions of sedimentary rocks. Various techniques are used in order to describe the diagenetic phases. Here, descriptions—seldom

quantitative, rather qualitative—are made on rock textures, primary sedimentary and diagenetic features as well as cements (in matrix and fractures/veins). Mineral replacements (e.g. dolomitization) and porosity are also investigated. A proper diagenetic study should lead to the following results: (i) identifying and defining the various diagenetic phases; (ii) organizing the diagenetic phases in chronological order—i.e. constructing a paragenesis (usually based on cross-cutting relationships and relative dating); (iii) inferring about the nature of original fluids that are responsible for the diagenetic processes and, subsequent, phases; and (iv) reconstructing the physico-chemical conditions that have prevailed during the respective diagenetic processes. Such results are inherent to develop conceptual models that explain the evolution of fluid-rock interactions and the sequence of diagenetic processes. Recently, this is also associated

with burial modelling in order to constrain the spatiotemporal settings of the diagenetic processes (e.g. Lopez-Horgue et al. 2010; Fontana et al. 2014; Peyravi et al. 2014).

Several techniques are commonly used when describing diagenetic phases in carbonate rocks. The classical ones are presented here.

2.1.1 Fieldwork

Whether the study concerns subsurface well cores or surface-exposed rocks, the first step consists of describing the accessible rocks and selecting representative samples for further, laboratory investigation. The field description of the diagenetic geo-bodies—sometimes of seismic-scale—(e.g. dolomite fronts) and facies (e.g. zebra dolomites) provides the basic building blocks for

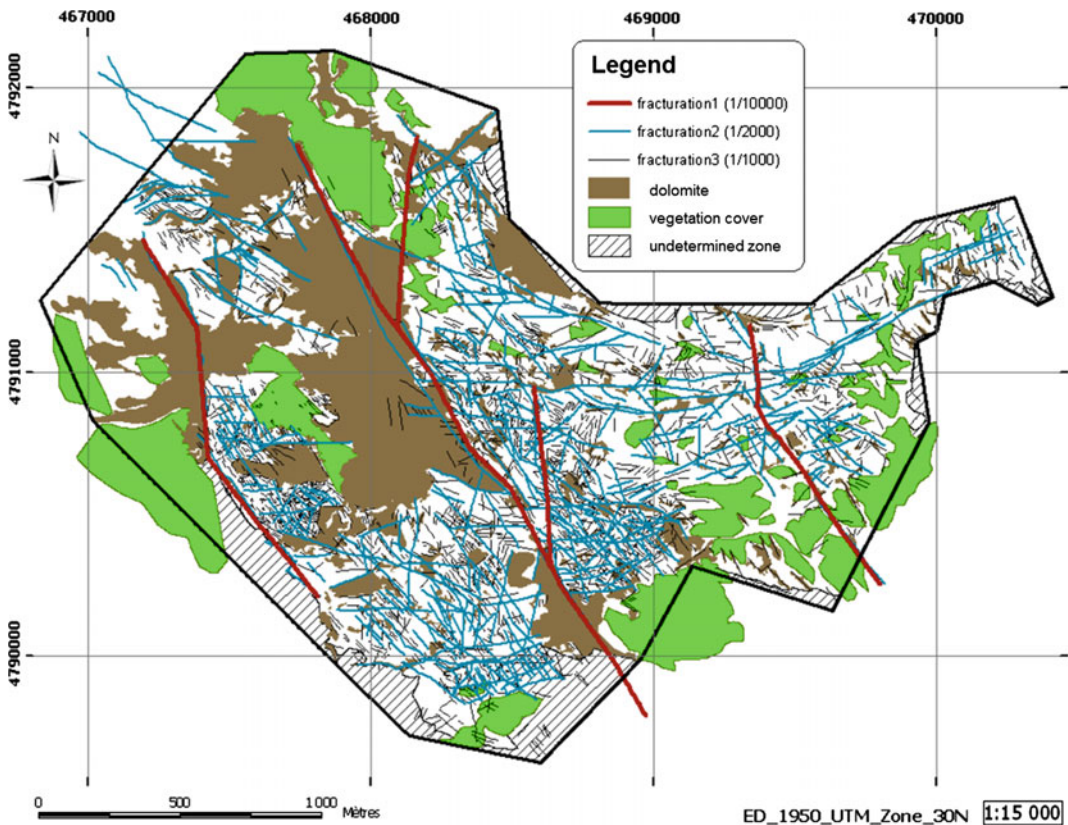


Fig. 2.1 Map showing dolomite occurrence and fracture (fault) lineaments in Cretaceous platform carbonate rocks exposed in Ranero (NE Spain), based on aerial photographs and fieldwork

any study. Here, mapping of diagenetic features is essential in order to understand the associated fluid-flow and the conceptual rock-fluid interactions (Shah et al. 2012; Nader et al. 2012; Fig. 2.1). In some cases, petrographic analyses can be achieved at the outcrop-scale (Fig. 2.2).

Many samples are usually collected by hammering pieces of rocks out of outcrops, whereas others are drilled out (with a micro-drillers) to retrieve detailed diagenetic cross-cutting features (e.g. distinct veins/fractures, stylolites) and/or to decrease the sample weight. Drilled samples are usually termed ‘plugs’, while hand-specimens are simply referred to as ‘samples’. When needed, oriented sampling is performed (i.e. measuring the sample position with respect to bedding and/or magnetic north). Table 2.1 lists the bulk material of a typical study—i.e. number of samples, thin sections, geochemical and mineralogical analyses, microthermometry and samples for crush-leach analyses. Sampling is

usually performed either vertically across stratigraphic columns, and/or laterally along sedimentological and/or diagenetic facies changes. It is usually planned on the m/cm scale across cross-cutting features considered to be of importance for the objectives of the study. For well-cores, detailed sedimentological logs are needed as background, based on which, sampling is performed.

2.1.2 Petrography

Petrographic analyses remain the basics of any diagenetic study. Carbonate rocks are investigated routinely with microscopic techniques to describe their textures, fabrics, and porosity. The various diagenetic features (replacive minerals, cements, dissolution, pressure-solution, etc.), are detailed and placed in chronological order based on cross-cutting relationships. Subsequently, a

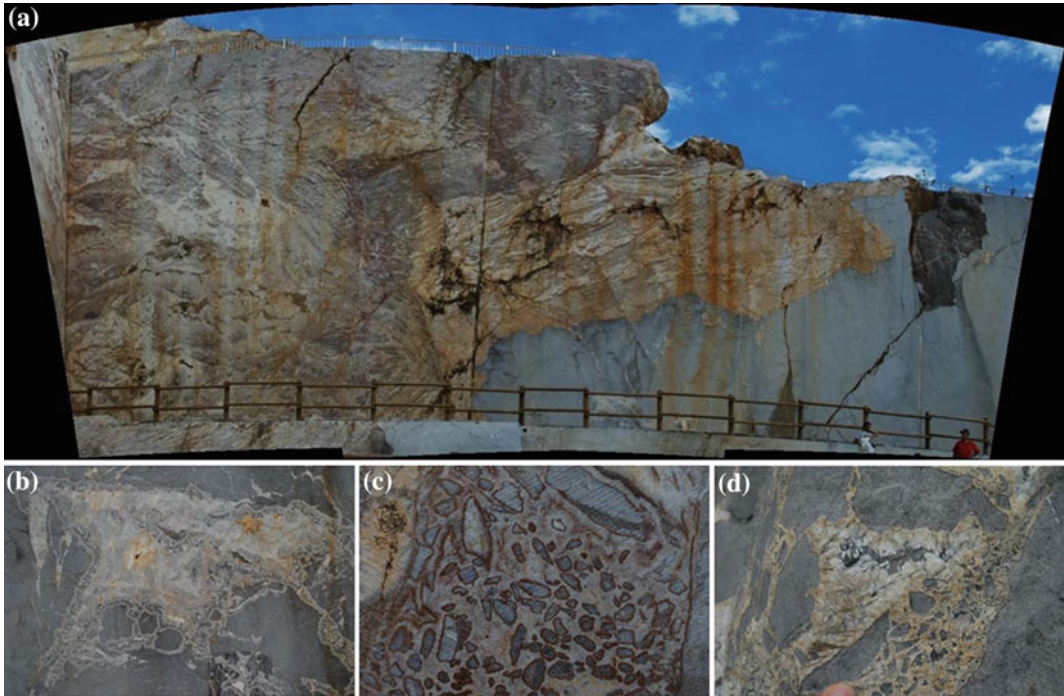


Fig. 2.2 Out-crop scale petrographic observations on the world class fault-associated dolomites in the Ranero, Pozalagua quarry/auditorium (NE Spain): **a** Overall view of the dolomite front in bluish-grey limestone;

b Cemented paleo-karst cavity in the limestone; **c** Limestone clasts in distinct dolomite cement phases; **d** Various calcite and dolomite cement phases

Table 2.1 Total list of material used throughout a typical diagenetic study (Nader 2003)

Sections locations	Samples (thin sections)	AAS	AES	O/C isotopes (sequential)	Sr isotopes	XRD	Wafers	Crush-leach
Jeita-Metn	226 (160)	140	14	125 (21)	19	33	8	12
N. Ibrahim	191 (106)	48		83 (2)	2	25	4	5
Qadisha	83 (32)	42		56		14		
Total	500 (241)	230	14	264 (23)	21	72	12	17

paragenesis is proposed and will be further refined with geochemical and mineralogical investigations as well as fluid inclusions analysis.

Samples are systematically subjected to preliminary preparation and ‘pre-microscopic’ observation (of cut-faces) before thin section preparation and subsequent conventional microscopic examination (Nader 2003). In general, plugs are less often processed through this scheme, and frequently anticipated to thin section preparation.

2.1.2.1 Pre-microscopic Observations

‘Pre-microscopic observations’ encompass a series of steps necessary for providing larger scale petrological information of a sample, and for efficiently locating representative two-dimensional thin sections. Accordingly, sample preparation first consists of sawing the pieces or plugs in order to produce flat cut-faces or ‘slabs’, which are then processed for polishing, etching, staining (and peeling, see Nader 2003), all combined with low magnification binocular macroscopic investigation. Staining carbonate rock slabs is usually done by applying a solution of potassium ferricyanide blue and alizarin red S (Dickson 1966). This is done in order to distinguish (ferroan) calcite and (ferroan) dolomite (Fig. 2.3). Other types of solution may be used to distinguish other minerals (e.g. feldspars, anhydrite/gypsum; e.g. Doummar 2005). The practical result of the ‘pre-microscopic’ procedures for each sample is to be able to decide whether thin section(s) is (are) to be prepared, and to choose the optimal location for the thin section(s).

When thin-sections are available for the study, best is to stain them (see above) and scan them with a high resolution scanner, in order to provide high-quality images for further quantitative measurements.

Recently the computerized tomography CT technique provides the possibility to scan bulk rocks (or well cores) in 3D in order to select the optimal sampling locations, before destroying the bulk sample. Then, smaller plugs can be drilled out of the bulk rocks and scanned with higher resolution. This technique should also be coupled with classical microscopic investigations.

2.1.2.2 Microscopic Observations

Thin sections are studied through conventional, fluorescence and cathodoluminescence microscopy (e.g. CL: Technosyn Cold Cathodoluminescence Model 8200 Mark II; operation conditions were 16–20 kV gun potential, 350–600 μ A beam current, 0.05 Torr vacuum and 5 mm beam width). Cathodoluminescence is simply the luminescence emitted by minerals when they are excited with radiation caused by an electron beam (Machel et al. 1991; Fig. 2.4). Microscopic viewing under fluorescent light can be used to investigate organic matter, to emphasis the porosity of carbonate rocks (impregnated with fluorescent dye), and to identify HC-rich fluid inclusions. Both fluorescence and cathodoluminescence (CL) microscopy should only be performed after the completion of conventional microscopic examination. Usually, for each CL and fluorescence photomicrograph a transmitted-light double is also taken. These

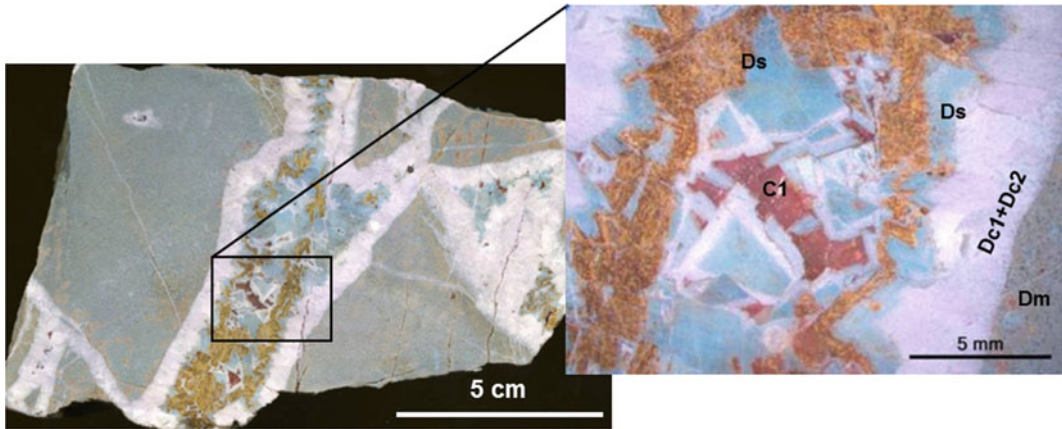


Fig. 2.3 Stained polished, etched slab of dolomite from the Ghalilah Formation (*Upper Triassic*) in Ras Al Khaimah (UAE), showing the host dolomite “Dm” together with fracture-filling non-ferroan (unstained)

dolomite cements (*Dc1* and *Dc2*) and a later phase of ferroan saddle dolomite cement (stained in blue, *Ds*), and a later calcite cement phase (*C1*), stained in red (from Fontana et al. 2014)

techniques proved to be very useful for pre-set targets (e.g. determination of specific cement types, emphasis porosity, comparison between similar diagenetic phases present in different samples, assessing the homogeneity of the sample for precise isotopic and/or chemical analyses).

Scanning electron microscopy (SEM) is a technique that allows the petrographic examination under three-dimensional viewing and higher magnifications (10–100,000 times). The relatively old JEOL-JSM 6400 Scanning Electron Microscope unit is an example of SEM devices with operating conditions of 15–40 kV accelerating voltage, $2 \cdot 10^{-7}$ to 10^{-9} A probe current, and working distance of 8–39 mm. The newer, EVO MA10 Zeiss SMT equipment has a

computer-motorized five axis stage, enabling rapid sample observation. It operates with a tungsten filament at 15 kV and 100 mA, and a probe current of 150–700 pA (for SE imaging and EDS analysis, respectively). Combined with an Energy Dispersive X-ray Spectrometer (EDS), relative determination of compositional elements, based on the X-ray energy, may be performed. The SEM works by producing a high energetic electron beam in vacuum (inside an electron gun; LaB₆ or tungsten filament) that is accelerated towards the specimen surface (Fig. 2.5). The electron bombardment of the specimen surface results in two types of electrons—low energy secondary electrons (SE) and high energy backscatter electrons (BE). The former electrons are captured in a photomultiplier tube and transformed into an image on the screen, while the latter backscatter electrons (BE) are used to detect compositional variations (given that the intensity of the BE is composition dependent, i.e. related to the mean atomic number of the target).

High resolution 2D compositional analyses are performed with new SEM-EDS (and/or micro-probes; EPMA) equipment (e.g. Zeiss EVO SEM, Oxford ESS), by applying punctual analysis for chemical composition and mineral mapping on thin-sections (Fig. 2.6). The time counting of 1000 microseconds can be set for spectral

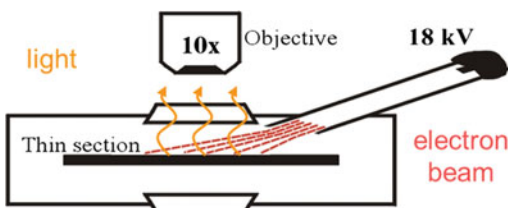


Fig. 2.4 A sketch showing the elementary constituents of cathodoluminescence (CL) microscopic technique: An electron beam focused on the upper face of a thin-section (or polished sample surface), which emits light (CL-pattern) that is observed under a microscope

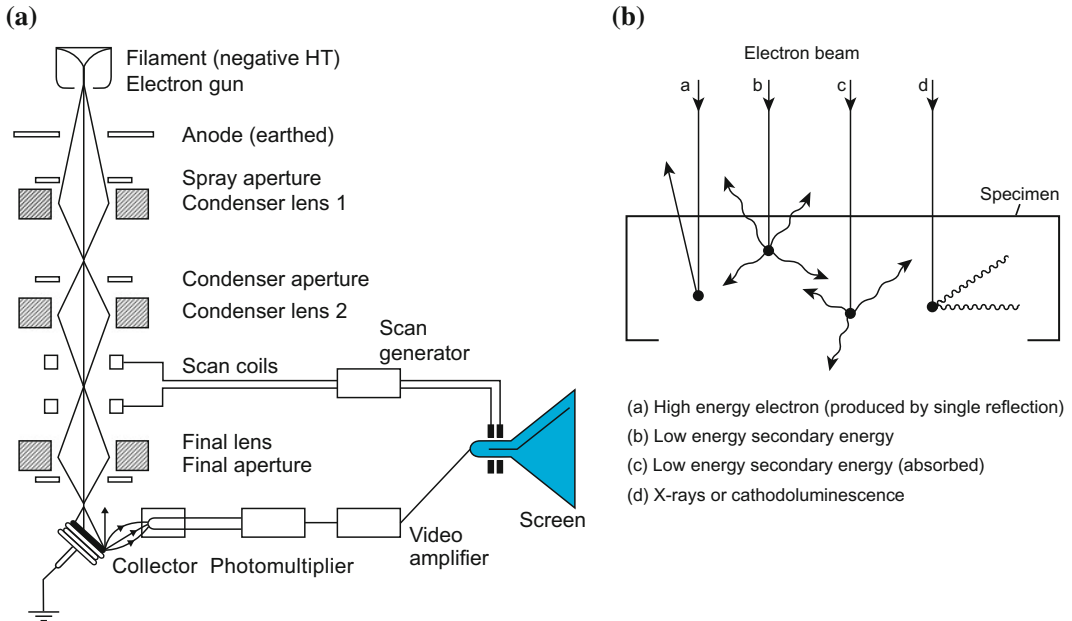


Fig. 2.5 Simplified illustration of the interior of a scanning electron microscope (SEM; **a**) and the resulting detected forms of energy (**b**). Sketch from Emery and Robinson (1993)

imaging, and the acquisition time for 86×128 pixels in the order of 1 h 30 min. Accordingly, mineral assemblages can be mapped, and the porosity change associated to mineralogical transformations through diagenesis can be determined. X-ray intensity maps of all elements are transformed to oxide wt.% by means of software packages (e.g. AZtecEnergy, produced by Oxford Instruments) constrained by EDS standardization. Statistical cluster analysis is commonly used to identify the different phases occurring in the samples (see below). Data output (from SEM-EDS analyses) can be further analysed with MatlabTM software based on De Andrade et al. (2006).

2.1.3 Geochemistry

A large variety of geochemical analyses are used in order to describe the chemical patterns of the diagenetic phases and to infer about the original fluids (at the time of precipitation or recrystallization). This quest remains very difficult and tricky due to the subtle “resetting” of the geochemical signatures of carbonate minerals

during diagenesis (e.g. Frisia et al. 2000). Only some of the major geochemical analyses that are routinely used for diagenesis studies are presented below.

2.1.3.1 Major and Trace Element Analyses

Major and trace elements allow defining the chemical characteristics of the diagenetic mineral phases, and eventually better constraining the fluid systems occurring during related diagenetic processes. Subsequently, they can also help in understanding the overall physico-chemical conditions and evolution through the proposed paragenesis.

Major and trace element analyses are carried out by flame Atomic Absorption Spectrometry (AAS), Atomic Emission Spectrometry (AES), and Inductively Coupled Plasma Mass Spectrometry (ICP-MS) which can be also coupled to a Laser Ablation device (LA-ICP-MS) to allow direct analysis of solid phases. In fact without Laser ablation, the rock samples need to be dissolved in solutions prior to analysis. Bulk samples (e.g. limestone/dolostone rock matrix), uni-phase samples (e.g. dolomite or calcite veins)

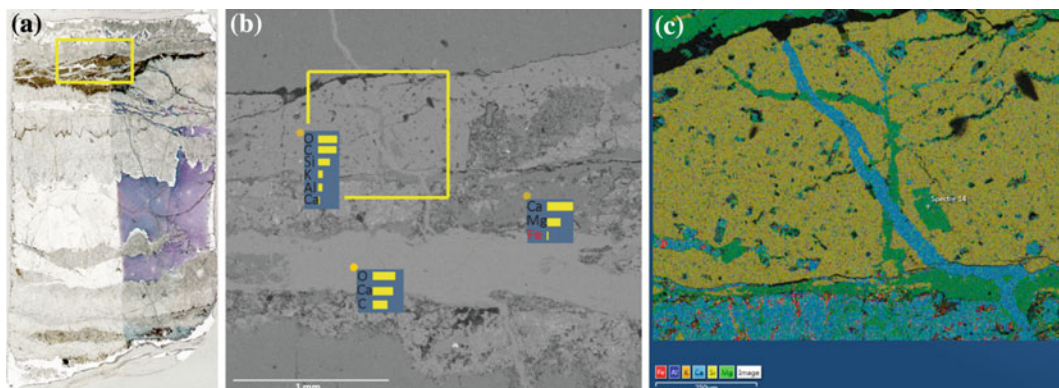


Fig. 2.6 Results of high resolution 2D elemental compositional SEM-EDS analysis performed on a stylolite in a dolostone from Latemar, northern Italy (courtesy of Katrine Blomme, KU Leuven): **a** stained thin-section with ferroan dolomite cement and clay-filled stylolite; **b** SEM photomicrograph showing a close-up view of the

yellow rectangle in (a) together with 3 spots of EDS analysis on clay, dolomite and calcite zones; and **c** EDS map of the area indicated by the yellow rectangle in **b**, showing a dolomite veinlet (rich in Mg) cross-cut by a calcite veinlet (rich in Ca) within the silica-rich clay of the stylolite

and multi-phase samples (e.g. dolomite/calcite of a calcitized dolostone) could be analysed by AAS (Fig. 2.7; Nader 2003; Maussen 2009). Due to their non-carbonate impurities and mixed volumes of calcite and dolomite, carbonate rocks are very problematic when it comes to determining their major and trace elemental distribution. The designed analytical procedures for sample preparation are the result of tedious trial and error lab-work.

2.1.3.2 IFPEN Protocol for AAS (Maussen 2009)

Flame atomic absorption spectrometry (AAS: Varian SpectrAA 240FS) is perfectly adequate to determine major and trace elements composition

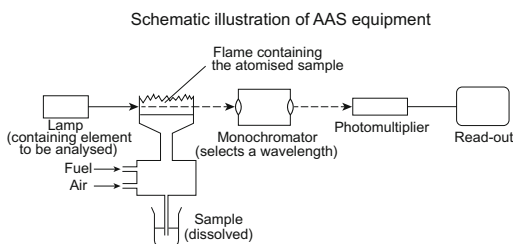


Fig. 2.7 Simplified diagram of AAS equipment and constituents—courtesy of Maussen (2009) (from A. Walsch: <http://www.hsc.csu.edu.au/chemistry/core/monitoring/chem943/943net.html>)

of sedimentary rocks (e.g. Ca, Mg, Fe and Mn contents among others). For major and trace element analyses, dolostone and limestone powdered samples (1 g of each) are leached in 40 ml (1 M) HCl and left on hot plates until evaporation. The residues are dissolved for a second time in 20 ml (1 M) HCl. Samples containing both calcite and dolomite are subjected to a sequential extraction procedure modified from Nader (2003) prior to geochemical analyses (Maussen 2009). Samples are leached in 60 ml of 4 %v/v. acetic acid to remove the calcite phase. After reaction, the remaining samples are evaporated. The residue is dissolved in 20 ml of 25 %v/v. nitric acid, the calcite evaporate is then dissolved with 20 ml of 25 %v/v. nitric acid. After filtering and rinsing, the resulting solution is considered to represent the calcite phase. The remaining solids (assumed to represent the dolomite phase and clays) are subjected to similar leaching procedures: dissolution in 20 ml of 25 %v/v. nitric acid, evaporation and dissolution in 20 ml of 25 %v/v. nitric acid. After filtering and rinsing, the resulting solution is considered to represent the dolomite phase and the remaining solids are clays. Calibration of the AAS needs to be achieved by means of a multi-element standard solution (in a 5 %v/v. nitric acid matrix). The multi-element standard solutions and sample

solutions are commonly matrix corrected for Ca and Mg. Analytical precision on ppm contents is generally less than 5 % for both mixed calcite/dolomite and dolomite samples.

2.1.3.3 Stable Oxygen and Carbon Isotopic Analyses

Oxygen and Carbon isotopic analyses help in shedding lights on the original type of fluids and temperature prevailing throughout diagenesis. Stable oxygen isotopes reflect the original fluids and the temperature during precipitation of the analysed carbonate phase. Thus, an independent argument is needed in order to estimate one of these two variables. Stable carbon isotopes are inherently related to the original seawater and soil-derived carbon. Often the $\delta^{13}\text{C}$ signature of the investigated diagenetic phase is buffered by that of the host-rocks (e.g. pointing towards its marine origin).

Stable isotope analyses are frequently done in specialized laboratories (e.g. Université Pierre et Marie Curie UPMC, Paris—France; Institute of Geology and Mineralogy, University of Erlangen—Germany). Samples are usually micro-drilled or micro-milled from the stained rock-slabs (or directly from thin sections), and sent to the qualified laboratory. The carbonate powders are commonly reacted with 100 % phosphoric acid (density > 1.9; Wachter and Hayes 1985) at 75 °C in an online carbonate preparation line (Carbo-Kiel—single sample acid bath) connected to a Finnigan Mat 252 mass-spectrometer. All values are reported in per mil relative to Vienna Pee Dee Belemnite (V-PDB) by assigning a $\delta^{13}\text{C}$ value of +1.95‰ and a $\delta^{18}\text{O}$ value of -2.20 ‰ to NBS19. Oxygen isotopic compositions of dolomites are usually corrected using the fractionation factors given by Rosenbaum and Sheppard (1986). Reproducibility based on replicate analysis of laboratory standards is better than ± 0.02 ‰ for $\delta^{13}\text{C}$ and ± 0.03 ‰ for $\delta^{18}\text{O}$.

For the samples that contain calcite and dolomite phases together (inseparable; e.g. dedolomite), a special double collection procedure can be performed (e.g. Nader et al. 2008). The same sample (about 10 μg , powdered) is first reacted with 100 % phosphoric acid for 2 h in a water-bath

at 25 °C. The extracted CO_2 is assumed to represent the calcite phase. Then, the reaction with the acid continues for 36 h (same operating conditions), or at higher temperatures (for a shorter time duration), before a second extraction of CO_2 considered to represent the dolomite phase.

2.1.3.4 Strontium Isotope Analyses

Strontium isotope ratios are usually used in order to determine either the age of the investigated diagenetic phase (compared to the evolution of the marine Sr curve; Fig. 2.8) or to infer about rock-fluid interactions (e.g. mixing and interaction with radiogenic Sr fluids).

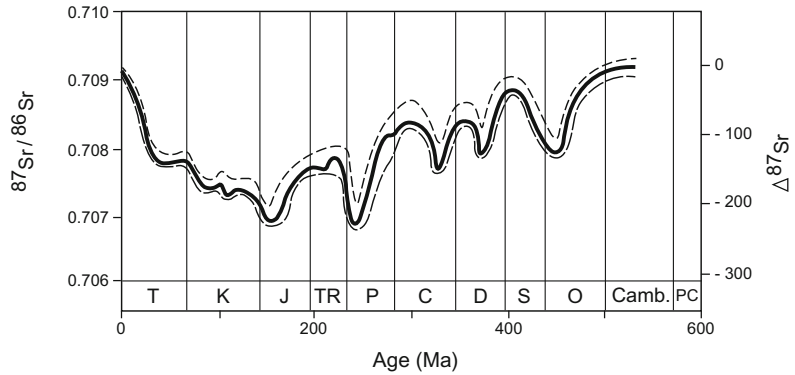
Sr isotope analyses are also carried out in specialized laboratories (e.g. BRGM, Orléans—France; SARN-CNRS, Nancy—France; SUERC, Glasgow—United Kingdom). Carbonate samples are leached in 1 M ammonium acetate prior to acid digestion. Calcite is digested in 1 M acetic acid, and dolomite in 6 M HCl. Sr is separated in 2.5 M HCl using Bio-Rad AG50W X8 200–400 mesh cation exchange resin. Total procedure blank for Sr samples prepared using this method is <200 pg. In preparation for mass spectrometry, Sr samples are loaded onto single Ta filaments with 1 M phosphoric acid. Sr samples are analysed on a VG Sector 54–30 multiple collector mass spectrometer. A ^{88}Sr intensity of 1 V ($1 \times 10^{-11}\text{A}$) ± 10 % is maintained and the $^{87}\text{Sr}/^{86}\text{Sr}$ ratio is corrected for mass fractionation using $^{86}\text{Sr}/^{88}\text{Sr} = 0.1194$ and an exponential law. The VG Sector 54–30 mass spectrometer is operated in the peak-jumping mode with data collected as 15 blocks of 10 ratios.

2.1.4 Mineralogy

Mineralogical investigations are usually done by means of X-ray diffraction (XRD) technique for various purposes: (i) determination of clay minerals, (ii) determination of amounts (%) of mineral phases in a rock (e.g. calcite, dolomite, anhydrite), and (iii) assessment of dolomite nonstoichiometry and crystal ordering.

The relative determination of calcite/dolomite percentage in a carbonate rock is possible by

Fig. 2.8 Variations of $^{87}\text{Sr}/^{86}\text{Sr}$ in seawater throughout the geologic time (from Emery and Robinson 1993). *Detached lines* represents the approximate limits of uncertainties



means of relative comparison of calcite/dolomite peak surfaces and Rietveld modelling. Optimized workflows have been designed based on several authors (e.g. Hutchison 1971; Roysse et al. 1971; Tucker 1988), and experimental laboratory work. Dolomite nonstoichiometry—mole (M) % CaCO_3 —is often calculated using the relationship between calcium content and $d_{[104]}$ spacing (Goldsmith and Graf 1958) and applying the equation of Lumsden to the measured $d_{[104]}$ spacing (Lumsden 1979):

$$N_{\text{CaCO}_3} = M d + B$$

where N_{CaCO_3} is the mole% CaCO_3 in the dolomite crystal lattice, d is the diffractogram's peak d spacing in Angstrom units, M is 333.33 and B is -911.99 .

Dolomite crystal ordering can be assessed by calculating the FWHM (full width of half maximum intensity) of the main dolomite peak on X-ray diffractograms. Experience showed that, within the context of relative assessment, this method yields better results than those of other traditional methods (described in Tucker 1988), where the surface area of the accessory dolomite smaller peaks are used to determine ordering ratios (Nader 2003). Jones et al. (2001) proposed a methodology for assessment of 'heterogeneous' dolostones, which exhibit multiple peaks and/or shoulders.

2.1.4.1 IFPEN Protocol for XRD (Turpin 2009; Turpin et al. 2012)

Small portions of each sample are uniformly ground in an agate mortar for XRD measurements.

Alumina from NIST is added to each powder sample for use as an internal standard (50 weight %) and the mixture is again ground until it becomes homogeneous. The Alumina cell parameters are taken from the NIST information (SRM 676a). XRD patterns are collected using Cu radiation with step size of $0.017^\circ 2\theta$ and counting time in the order of $91 \text{ s} \cdot 2\theta^{-1}$ (with a position-sensitive detector on an X'pertPro Analytical diffractometer). The identification of minerals is performed on the measured digitized diffractograms, using the ICDD database (PDF4+). XRD analyses in $\theta-2\theta$ configuration is performed with a parallel beam focused by an elliptic W/Si crystal mirror. The measurements are undertaken on the powder samples enclosed in a 1 mm glass capillary, to enable the analysis of the whole sample.

Structure and cell refinements are then performed on the resulting diagrams. The structure refinement method (Rietveld 1969) is based on a least-squares refinement procedure which employs directly the profile intensities obtained from step-scanning measurements of the powder diagram. It allows making some quantitative judgment of the agreement between observed and calculated integrated intensities instead of profile intensities. A fair approximation to the observed integrated intensities can be made by separating the peaks according to the calculated values of the integrated intensities. Based on all diffraction peaks, the Rietveld refinement is used to quantify the relative proportions of coexisting phases in samples and cell refinement, to determine the unit cell parameters of the dolomite crystals. The peak positions of the NIST Alumina

are used to correct the peak shift error (in two-theta) for the various constituent of each sample between experimental and calculated profiles. The relative error on quantification via Rietveld refinement has been already calculated for common minerals. The uncertainty is logically linked to the phase proportion in the sample: when abundance is <5 %, uncertainty is >75 % while it is <10 % when proportion is >80 %.

2.1.4.2 Electron Microprobe

Electron microprobe analyses (EMPA) are usually undertaken only on key samples. Their use aims to map mineralogical assemblages (and possible evidence of incorporated Fe and Mn in the carbonate minerals). EMP (mapping) analyses are achieved using a Cameca SX100 microprobe under the following analytical conditions: 15 kV, 100nA, 0.3 s for all analysed elements (e.g. Ca, Mg, Fe, Mn, Sr), with 1 μm spot size and 5 μm step size.

The electron microprobe is standardized on diopside for magnesium and calcium, garnet for iron, rhodonite for manganese and celestine for strontium. X-ray intensity maps of all elements were transformed into oxide weight% concentration maps according to the procedure of De Andrade et al. (2006), using high quality point analyses. A statistical cluster analysis could identify the different major mineral phases occurring in the samples. For carbonate clusters, a structural formula is calculated for each pixel using a 1 oxygen basis, and assuming all iron to be divalent (Fig. 2.9). The maps of structural formulas are then filtered to remove pixel analyses located at the limit between different homogeneous phases (mechanical mixing on contaminated analyses). The remaining structural formulas were filtered using the following equations: (i) $0.96 < \text{Ca} < 1.14$; (ii) $0.86 < \text{Mg} < 1.04$; and (iii) $0.0 < \text{Fe} < 0.1$ (per formula unit with 0.1 as standard analytical error). This set of constraints are defined by natural variation of typical dolomite compositions between two end members; i.e. $\text{Ca}_{0.96}\text{Mg}_{1.04}(\text{CO}_3)_2$ and

$\text{Ca}_{1.14}\text{Mg}_{0.86}(\text{CO}_3)_2$ calculated for 48 and 57 % dolomite nonstoichiometry, respectively.

2.1.5 Fluid Inclusions

Analyses of fluid inclusions trapped in diagenetic minerals (and cements) provide one of the few tools that allow a direct reconstruction of the thermal and fluid composition history of a sedimentary basin (e.g. Ceriani et al. 2002; Swennen et al. 2003; Nader et al. 2004).

2.1.5.1 Microthermometry

Microthermometric analyses of fluid inclusions are performed on double-polished sections using a Linkam THMSG 600 heating cooling stage mounted on an Olympus BX60 microscope. The liquid-vapor homogenization temperatures (T_h) of two-phase primary and pseudo-secondary aqueous fluid inclusions are studied in order to estimate the temperature of precipitation for the host crystal. Assuming that the investigated minerals derive from a certain fluid system (such as $\text{NaCl-H}_2\text{O}$), the final melting temperatures of ice (T_m) are used to infer about the salinity of the fluid itself (Fig. 2.10). Measurement accuracy is usually in the order of 1 $^\circ\text{C}$ for T_h values and 0.2 $^\circ\text{C}$ for T_m values. T_h values are also used in association with $\delta^{18}\text{O}$ isotopic data in order to reconstruct $\delta^{18}\text{O}$ composition of the parent fluids.

2.1.5.2 Crush-leach Analyses

Specific sample phases are carefully cut from core or hand sample using a saw and then cleaned with a dentist's drill, mainly representing phases whose fluid inclusions were properly investigated. The samples are crushed and sieved to give a 1–2 mm grain size fraction and hand-picked under a binocular microscope to obtain 2 g of a clean mineral separate where possible. The samples are then washed in 18.2 ml water, heated overnight on a hot plate, electrolytically cleaned for 1 week and then dried in an oven. 1–2 g of sample are ground to a fine

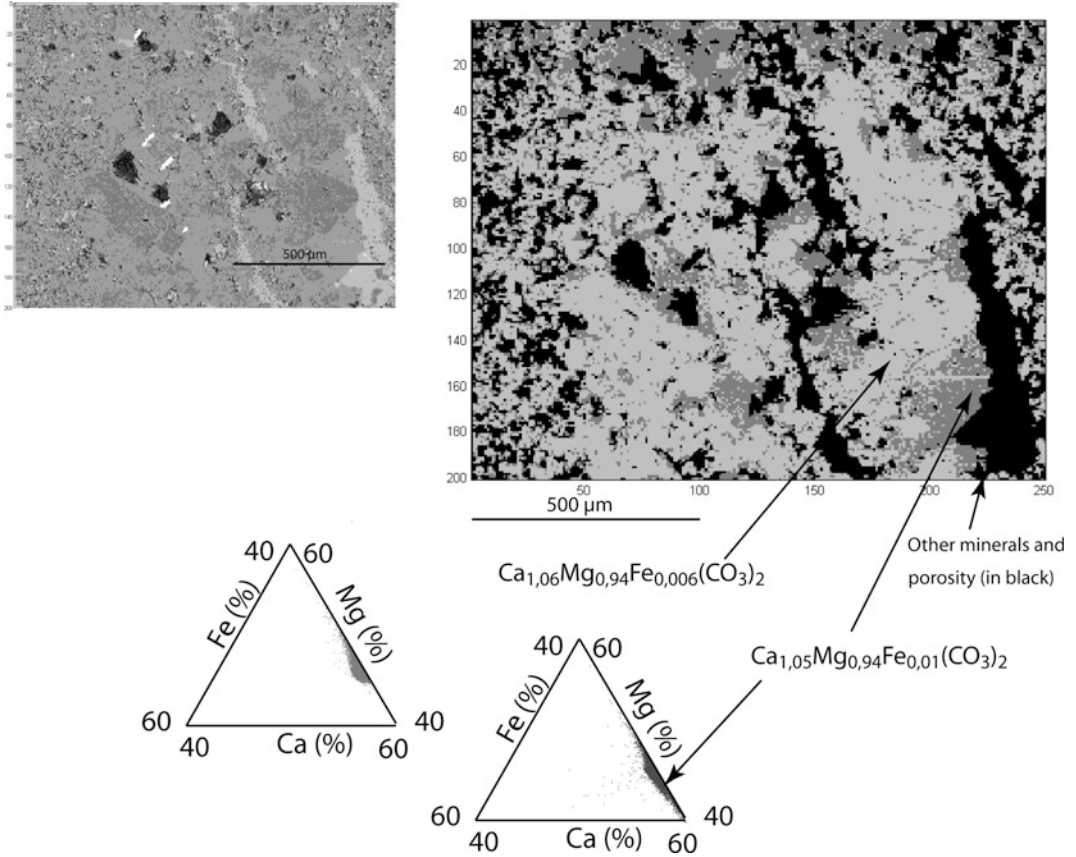
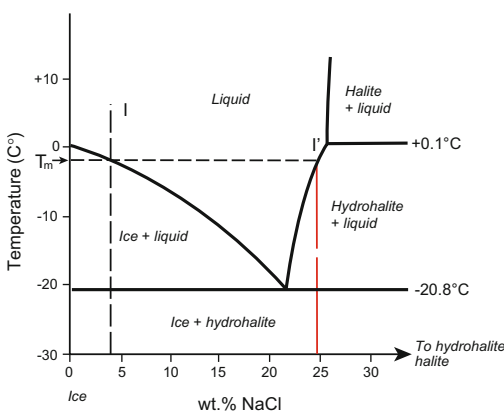


Fig. 2.9 SEM backscattered electron image (left) and cluster analysis of electron microprobe map (right), as well as mean structural formula for two different dolomites with varying chemical composition in Ca–Mg–Fe ternary diagram. Triassic dolomite rock sample (well core) from the French Jura (Turpin 2009)



Dissolved species	Eutectic temperature (°C)	Eutectic composition (wt. %)	Solid phases		
			H ₂ O	ice	hexagonal colorless RI e 11.3 w 1.30
NaCl	-20.8	23.3% NaCl	aCl ₂ H ₂ O	hydrohalitem	monoclin/ice colorless RI 1.416
			NaCl	halite	cubic colorless RI 1.544
KCl	-10.6	19.7% KCl	KCl	sylvite	cubic colorless yellowish RI 1.490
CaCl ₂	-49.8	30.2% CaCl ₂	CaCl ₂ ·6H ₂ O	antarcticite	exagonal colorless RI e 1.39 w 1.41
MgCl ₂	-33.6	21.0% MgCl ₂	MgCl ₂ ·12H ₂ O		
NaCl-KCl	-22.9	20.17% NaCl 5.81% KCl			
NaCl-CaCl ₂	-52.0	1.8% NaCl 29.4% CaCl ₂			
NaCl-MgCl ₂	-35.0	1.56% NaCl 22.75% MgCl ₂			
NaCl-CaCl ₂ -MgCl ₂					

Fig. 2.10 Typical phase diagram for NaCl–H₂O fluid systems and selected phase data for aqueous solutions of chloride species commonly found in fluid inclusions (modified from Emery and Robinson 1993)

powder in an agate mortar and pestle in a clean and controlled environment. Half the powder is transferred to an unreactive vial and 5 ml of clean water was added. These samples are shaken, and filtered through 0.2 micron filters to give a clean leachate. Anions (Cl, Br, F and sulfate) are analysed using a Dionex DX600 ion chromatograph or ICP-MS (see above). Na and K and other cations are analysed on the same leachate using atomic absorption spectroscopy or ICP-MS.

2.1.6 Integrated Techniques for Building Conceptual Models

Through the application of various techniques, independent arguments are collected to describe the diagenetic features and organize the respective phases (and processes) in chronological order. Hence, a paragenesis can be presented, and

it is commonly associated with a porogenesis (evolution of porosity, see above). It spans the time since the deposition until burial and/or surface exposure—practically until sampling took place (Fig. 2.11).

Each of the documented diagenetic phase represents a certain process that is pigeon-holed in a diagenetic realm with specific physico-chemical conditions. Then a conceptual model could be associated with the defined process. Based on detailed petrographic analyses with geochemical characterization of the key diagenetic phases and fluid inclusion analyses, Nader et al. (2007) constructed the paragenesis of a hydrothermal dolomite front in Jurassic platform carbonate rocks. The cross-cutting relationships as well as the petrographic and geochemical characteristics of the dolomite phases helped in relative-dating the process of front emplacement. Accordingly, a conceptual model could be presented illustrating the spatial/temporal evolution of the hydrothermal dolomite front (Fig. 2.12).

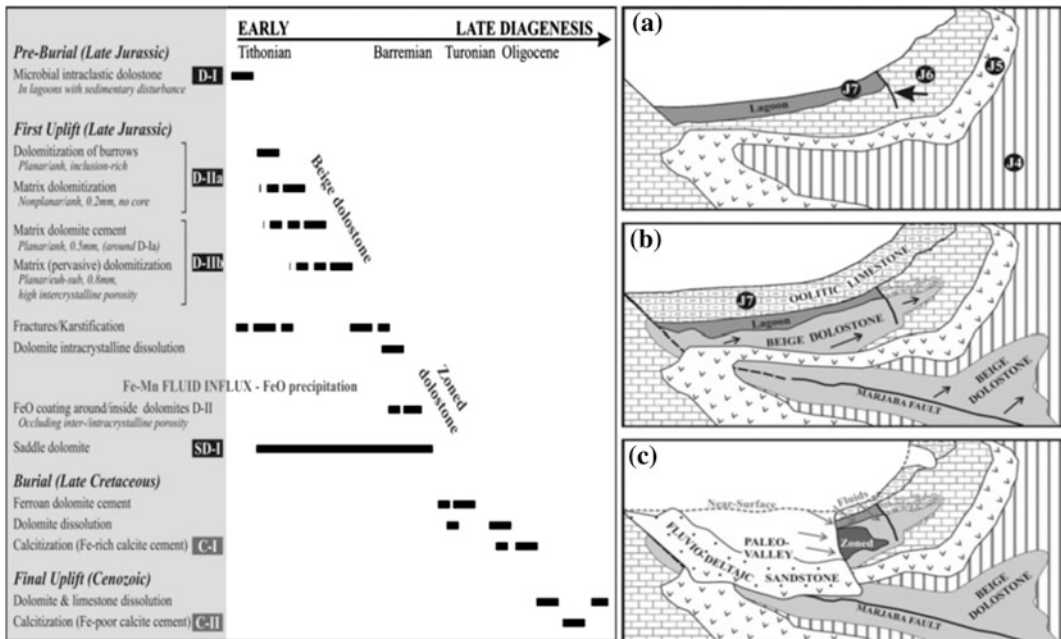


Fig. 2.11 Proposed sequence of diagenetic phases (paragenesis) for the dolostones of the Marjaba HDT front (central, Lebanon) based on petrographic, geochemical and fluid inclusion analyses. Cartoons a–c represent the proposed conceptual model of the dolomite front

emplacement and evolution (beige dolomite, ferroan zoned dolomite, dolomite cementation/dissolution) during the Kimmeridgian-Tithonian, Tithonian-Early Cretaceous, and early Cretaceous, respectively (Nader et al. 2007)

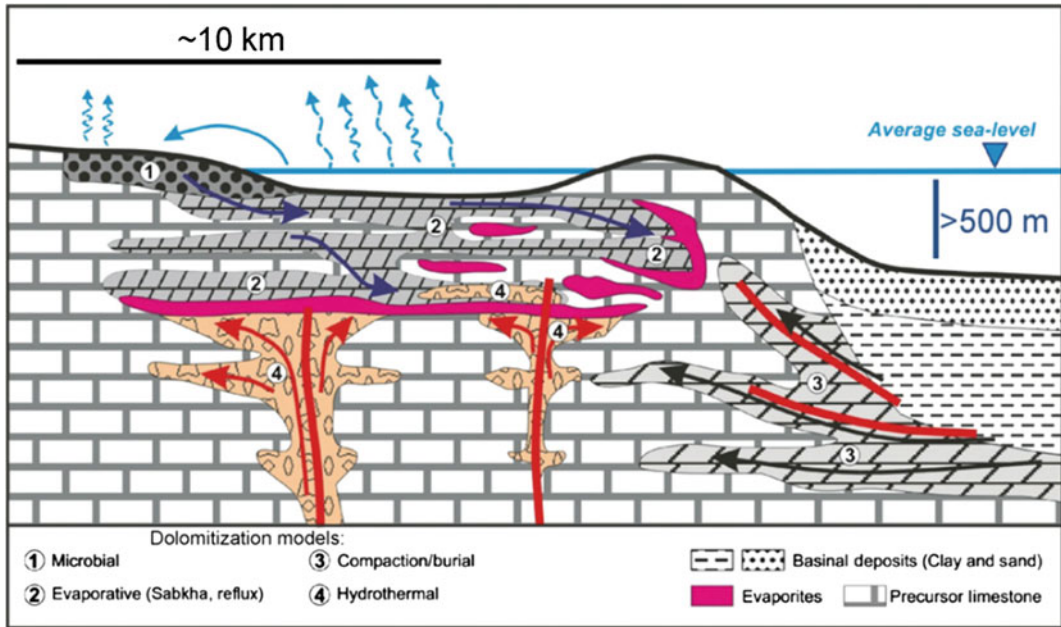


Fig. 2.12 Examples of conceptual dolomitization models and their schematic geometries and extent. The expected fluid flow pathways are indicated with *arrows* (from Nader et al. 2013)

Alternatively, reflux, burial or fracture-related dolomitization models (Fig. 2.12) may be invoked to explain a certain dolomite phase, whose petrographic and geochemical characteristics have been detailed. By following similar workflows, and through the comparison with other similar study cases, further constraints on the geometry (extent) and timing of the process may be reached. In addition, the hydrodynamic settings during the operation of such process may be proposed. The spatial heterogeneity in the host rock is eventually qualitatively estimated together with the impacts on reservoir properties (namely, porogenesis).

2.2 Future Perspectives

At this stage, it is fair to state that the various characterization methods for diagenesis and overall workflows are well advanced. Additional analytical techniques will certainly bring more precision and better constrains to diagenesis, namely through quantitative techniques. Indeed, some new, promising analytical techniques are

currently being developed, building up further the state of the art of diagenesis studies (e.g. clumped oxygen and magnesium isotopic analyses). In addition, new cutting edge technologies in investigating porosity will undoubtedly bring a new era. Until today, the analyses of porosity in sedimentary rocks often is based on the rock textures—see above, the classifications of Choquette and Pray (1970) and Luccia (1995) and Lønøy (2006). The coming years will probably reveal another approach to understand the porosity evolution by focusing on the investigations of the pore space itself. This is becoming possible through advances in computed tomography techniques capable of capturing the porous space in 3D at the macro-scale (intergranular) and micro-scale (intra-granular).

2.2.1 Clumped Oxygen Isotopic Analyses

Oxygen stable isotopic analyses infer about the nature of the original fluids and the temperature during precipitation of carbonate minerals. Such

results are hindered by two variables (original fluids chemistry and precipitation temperature, as presented above). Fluid inclusions analyses are often used as an independent approach to constrain the precipitation temperatures, and, together with stable oxygen isotopic results, confirm the original nature of the precipitating fluid. Yet, carbonate rocks in general (and dolomites in particular) have fluid inclusions that often are damaged by leakage or stretching. A new paleo-thermometer is therefore needed, one that can be used on several types of cement fabrics/types, and that is not associated to any other unknown variable. The ‘clumped’ oxygen isotopic analyses are believed to provide such paleo-thermometry approach, and are expected to have great analytical potentials in the near future.

While the classic stable isotopic analyses (e.g. $\delta^{18}\text{O}$, $\delta^{13}\text{C}$) aim to estimate the difference between the isotopes’ ratio (e.g. $^{18}\text{O}/^{16}\text{O}$, $^{13}\text{C}/^{12}\text{C}$) of the rock sample compared to that of an international standard, the ‘clumped’ isotopic analyses distinguishes specific ‘isotopologues’—i.e. molecules of similar chemical composition but different isotopic composition. Practically, the isotopologue of CO_2 with a mass of 47—i.e. $\Delta 47$ —(where the heavy, rare isotopes of carbon and oxygen, ^{13}C and ^{18}O , are substituted in the CO_2 molecule; i.e. $^{13}\text{C}^{18}\text{O}^{16}\text{O}_2^{2-}$) is measured representing the amount of ‘clumping’ of the heavy isotopes in the crystal lattice (Fig. 2.13). This is achieved by simultaneous measurement of $\delta^{18}\text{O}$ and $\delta^{13}\text{C}$ to $\Delta 47$ in the same sample, with no comparison with external references.

The amount of ‘clumping’ can be known at a specific temperature according to the laws of thermodynamics. Ghosh et al. (2006) demonstrated that a single calibration line could be derived for the $\Delta 47$ values of different carbonate minerals that have precipitated at distinct temperatures (Fig. 2.14; Eiler 2007). Hence, ‘clumped’ isotopes are free of mineral specific fractionation effects in contrast to $\delta^{18}\text{O}$ and $\delta^{13}\text{C}$ measurements. $\Delta 47$ is independent of the original fluid $\delta^{18}\text{O}$ composition; it only reflects temperature.

Accordingly, the carbonate ‘clumped’ isotope paleo-thermometry is based on the temperature-

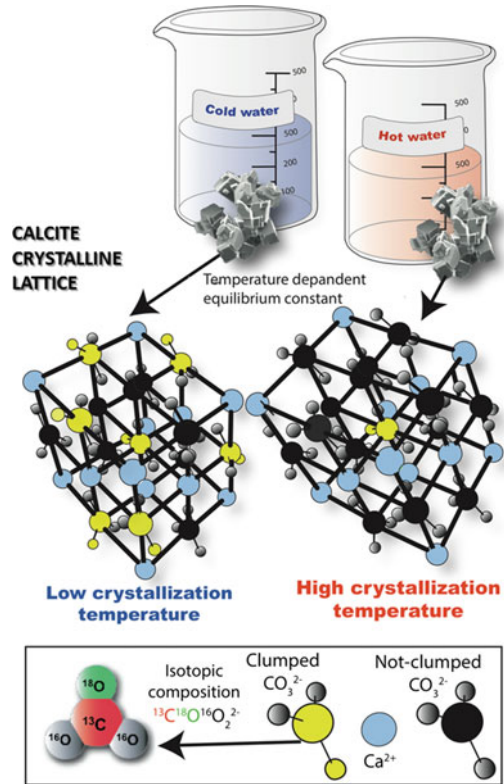


Fig. 2.13 The amount of “clumped” oxygen isotopes is calculated by the measuring the quantity of $\Delta 47$ isotopologues of CO_2 in a calcite lattice (i.e. $^{13}\text{C}^{18}\text{O}^{16}\text{O}_2^{2-}$), which is a function of temperature of crystallization (illustration courtesy of Xavier Mangenot, IFPEN 2015)

dependent formation of an isotopologue of CO_2 with a mass of 47 within the carbonate minerals ($^{13}\text{C}^{18}\text{O}^{16}\text{O}_2^{2-}$ ionic groups, as presented above). This is done by determining $\Delta 47$ values of CO_2 extracted from the minerals, and comparing results with the temperature calibration line.

More recently, analyses of clumped isotopes have been made possible and standardized for calcite and dolomite (e.g. Dennis et al. 2011). Henceforth, estimations of the crystallization temperatures of diagenetic calcites at temperatures varying from 14 to 123 °C (Huntington et al. 2011) and synthetic dolomites at temperatures between 25 and 350 °C (Bonifacie et al. 2013, 2014), have been achieved and published. The calibration lines for calcite and dolomite are currently being improved with additional

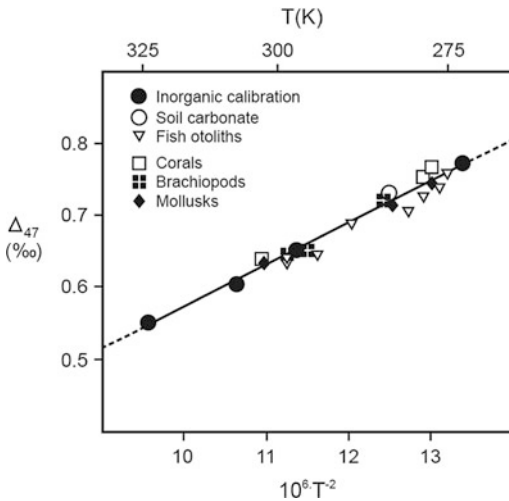


Fig. 2.14 Interpolated (solid) line of Δ_{47} values (in ‰) and corresponding temperatures (in K) for inorganic and organic carbonates (from Eiler 2007)

published data (*pers. communication* Xavier Mangenot, IFPEN 2015).

2.2.2 Mg Isotopic Analyses

Magnesium (Mg) is a major rock-forming element in terms of its abundance (second, after oxygen). It is ubiquitously present in the seawater, where most of carbonate rocks are formed. It is also present in the hydrological and biological systems (Young and Galy 2004). The multiple-collector inductively coupled plasma-source mass spectrometers (MC-ICP-MS) is capable to properly measure the Mg isotopic ratios $^{25}\text{Mg}/^{24}\text{Mg}$ and $^{26}\text{Mg}/^{24}\text{Mg}$ in dissolved samples (e.g. Young and Galy 2004). Besides thermal ionization mass spectrometry (TIMS) allows precise measurements of the differences in $^{26}\text{Mg}/^{24}\text{Mg}$ from a fixed “terrestrial” value.

Li et al. (2012) measured the Mg isotope fractionation between Mg-bearing calcite and Mg in aqueous solutions over a range of temperatures (4–45 °C). Their results, together with those of other workers (e.g. Schauble 2011; Rustad et al. 2010) allowed to constrain furthermore the Mg isotope fractionation factors between carbonates and solution (see Fig. 2.15). They have also

demonstrated that the $\Delta^{26/24}\text{Mg}_{\text{cal-sol}}$ fractionation is insensitive to $p\text{CO}_2$, solution chemistry, and calcite composition, and that it is only slightly affected by temperature. Therefore, the Mg isotopes can be used to constrain Mg fluxes (including continental weathering) in modern and ancient marine systems.

Mg isotopic compositions of carbonate minerals could be compared to the $\delta^{26}\text{Mg}$ of modern carbonates, and become of interest for diagenesis studies (e.g. Lavoie et al. 2011; Li et al. 2012). For instance, they can offer important insights into the sources of Mg (necessary for the dolomitization processes), and thus, they can validate some conceptual models of dolomitization (Fig. 2.16). Often $\delta^{26}\text{Mg}$ isotopic analyses are done after securing other classical geochemical analyses (e.g. $\delta^{18}\text{O}$, $\delta^{13}\text{C}$, $^{87}\text{Sr}/^{86}\text{Sr}$) and fluid inclusions. Lavoie et al. (2011) revealed

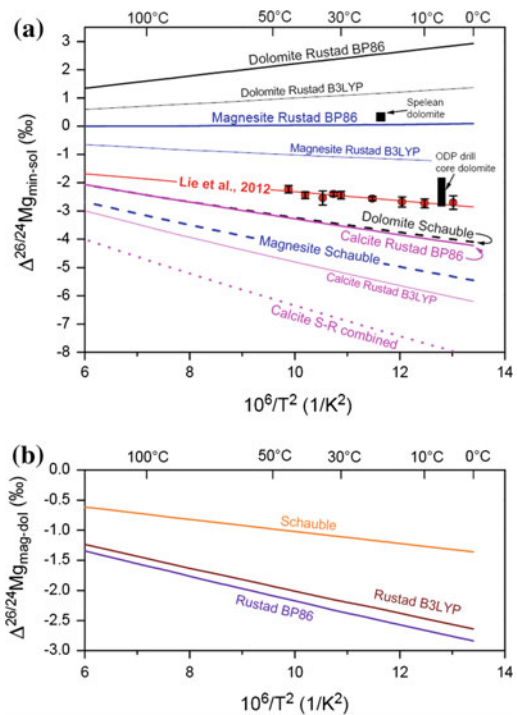


Fig. 2.15 Theoretically predicted Mg isotope fractionation factors (from Li et al. 2012 and references therein): **a** Mg isotope fractionation factors between carbonates and solution with respect to temperature. **b** Mg isotope fractionation factors between magnesite and dolomite relative to temperature

linear relationships between the $\delta^{26}\text{Mg}$, $\delta^{18}\text{O}$, and $^{87}\text{Sr}/^{86}\text{Sr}$ values for the Paleozoic dolomites of eastern Canada. Accordingly, they were able to constrain the nature of the dolomitizing fluid and its probable source from mafic and ultra-mafic volcanic rocks.

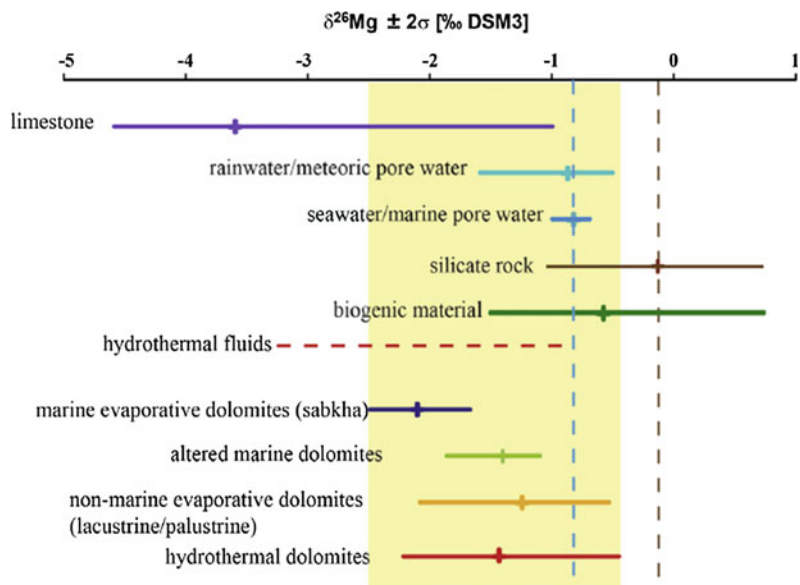
2.2.3 U-Pb Dating

U-Pb dating method of carbonate minerals is actually applicable to almost the entire geologic time scale, while it was previously somehow restricted to Pleistocene speleothems (e.g. Verheyden et al. 2008). Smith et al. (1991) succeeded U-Pb radiometric age determination of secondary calcite phases in Middle Devonian carbonate rocks and corals (Ontario, USA), paving the way to direct dating of carbonate diagenesis. Advanced technology for the new versions of MC-ICP-MS coupled with laser ablation, and the new thermal ionization mass spectrometers (TIMS) allowed higher precision and adequate measurements even if the U and Pb quantities are minute in the investigated samples. Thus, U-Pb dating has been undertaken successfully on carbonates from a broad range of depositional and diagenetic environments.

Rasbury and Cole (2009) presented the state of the art in terms of laboratory techniques and analytical protocols for achieving U-Pb dating on carbonate minerals. There is no doubt that this method has a great potential for dating diagenetic phases and inferring related processes.

Grandia et al. (2000) succeeded in U-Pb and Th-Pb dating of carbonates that are associated with Mesozoic MVT ore deposits. Since, most carbonates are somehow affected by diagenetic alterations, the main difficulty in applying such radiometric isotope dating is in distinguishing the time of formation of the deposit from its diagenetic alteration (Jahn and Cuvellier 1994; Rasbury and Cole 2009). This relies more on the petrographic investigations—and other diagenetic characterization techniques—than on the precision of radiometric dating. Indeed, the U-Pb dating technique abides by the necessary considerations common to most of used radioisotopic systems for dating. These are: (i) daughter isotopes are initially homogeneous; (ii) parent/daughter ratios are well spread; (iii) relevant half-life decay of the parent [with respect to the measured age]; and (iv) prevailing closed system. In addition, some problematic issues have to be taken into consideration when applying U-Pb dating for carbonates (Jahn and Cuvellier 1994):

Fig. 2.16 Magnesium isotopic composition ($\delta^{26}\text{Mg}$ DSM3) of different Mg sources (e.g. limestones, seawater, rainwater, silicate rocks, plant material), as well as resulting sabkha-, mixing zone and lacustrine dolomites (from Geske et al. 2015)



(i) U-Pb incorporation during carbonate rock deposition/formation; (ii) identification of the U-carriers in the carbonates; (iii) time interval between deposition and diagenesis as mentioned above (e.g. dolomitization); and (iv) diagenesis influence on Pb isotopic homogenization and U-Pb redistribution.

The resulting isochrones represent, for a specific age, the parent-daughter ratio on x-axis while the y-axis shows the ratio of the daughter isotope over the same denominator used for the x-axis (Fig. 2.17).

More recently, Li et al. (2014) undertook U-Pb dating on early calcite cements in Mesozoic ammonites with LA-ICP-MC-MS

technique. The analyzed cements resulted in U-Pb ages that are close to 159 Ma (Fig. 2.18a) and 165 Ma (Fig. 2.18b, c), about 10 and 15 Myr younger than the Bajocian and Toarcian strata where the ammonites are found, respectively (the stratigraphic intervals have numerical ages of 168.3–170.3 Ma, and 179–180 Ma; Gradstein et al. 2012). Li et al. (2014) interpreted the measured ages to be the time at which the walls and internal structures of the ammonites as well as the early-diagenetic fringing cements inverted from aragonite to calcite and distributed their uranium content into the fringing cements as they recrystallized during late diagenesis. This study shows the subtlety of this method and the necessity to interpret the produced analytical results with critical reasoning, taking into consideration other independent arguments.

2.2.4 3D Porosity

The flow properties of carbonate rocks are difficult to characterize, and to subsequently predict. Various classifications attempt to associate different types of porosity (partially based on the textures of rocks and their constituents) with measured permeability values (e.g. Lucia 1995; Lønøy 2006). Statistical analyses are usually performed on industrial well cores data-bases of thin section porosity typing with the corresponding flow properties measurements (e.g. MICP, Air-Permeability, Helium-Porosity). These analyses lead to rock-typing throughout the investigated reservoirs, which is a necessary step for reservoir-modelling. Subsequently, reservoirs are subdivided into zones with specific porosity/permeability characteristics (among other properties).

The current applied workflow for classical reservoir rock-typing is about to evolve with the advances in X-ray computed tomography capable of providing high resolution, three-dimensional imaging of the pore networks. Micro-CT approach coupled with 3D-image analyses allow, indeed, the characterization of the pore space in 3D irrespectively of the rock

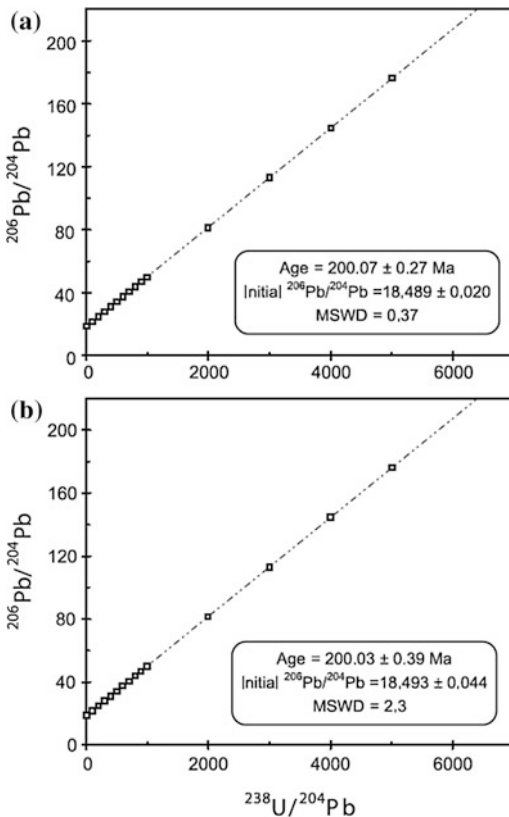


Fig. 2.17 Examples of isochrones evolved to a same age, i.e. 200 Ma from both, homogeneous (a) and heterogeneous (b) starting conditions. These results show demonstrate that “correct” ages can be obtained even with initial scatter in Pb isotopes (represented here by higher MSWD values; from Rasbury and Cole 2009)

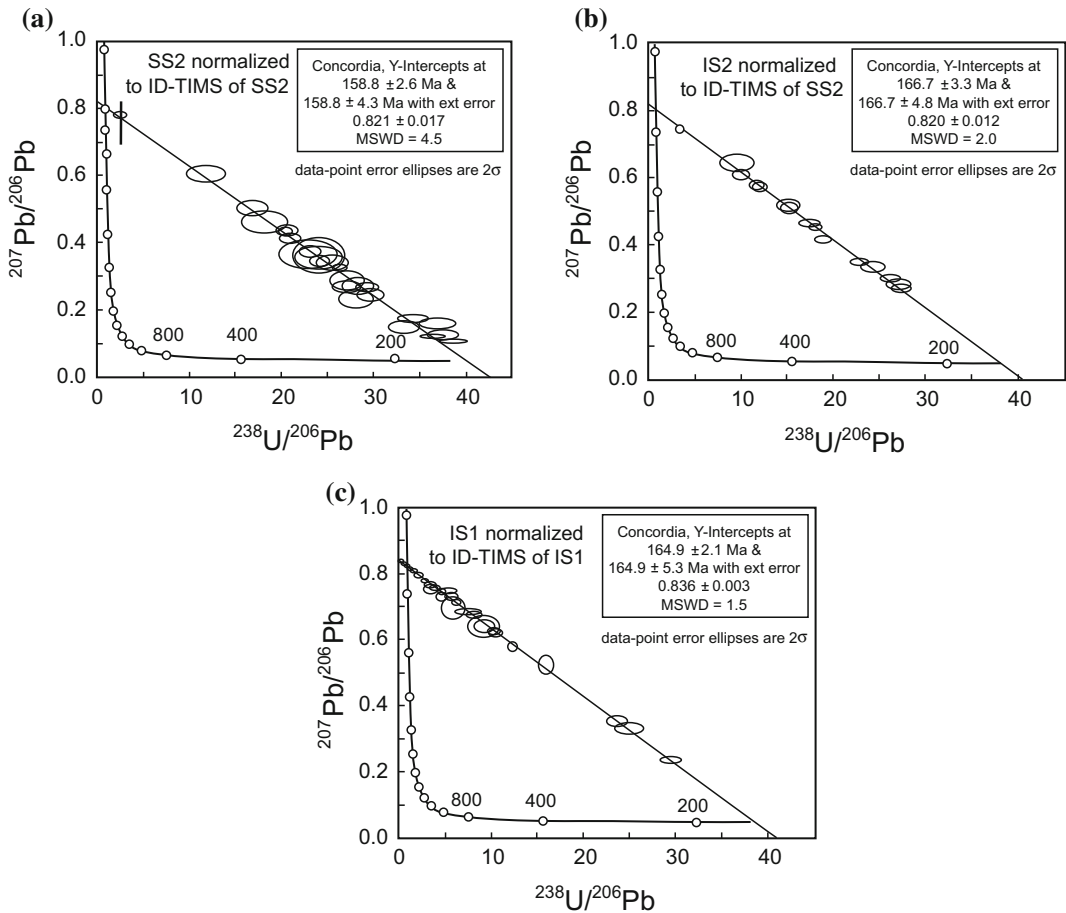


Fig. 2.18 Diagrams of LA-ICP-MS-Pb data that has been normalized to TIMS measurements of early calcite cement in Jurassic ammonites (from Li et al. 2014). See text for details

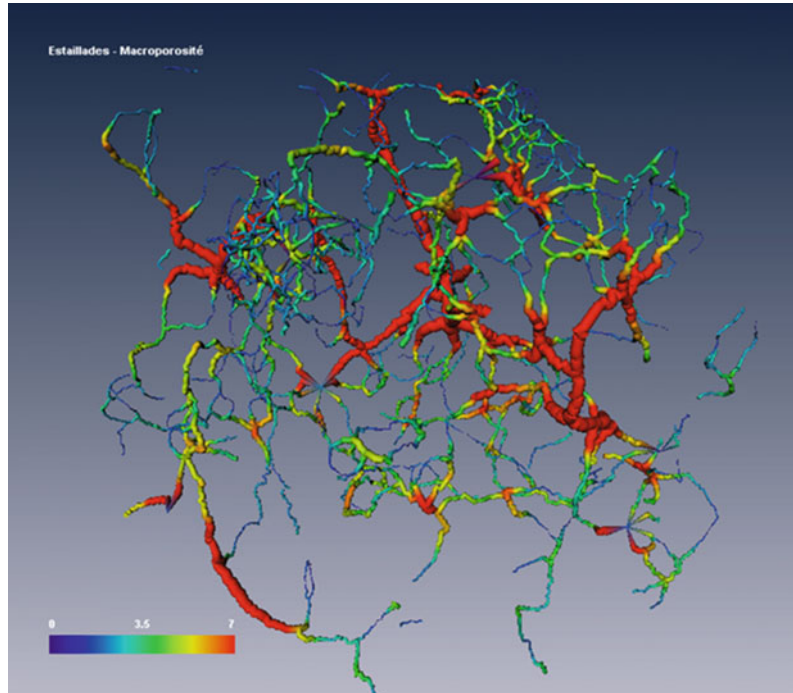
texture itself. Porosity becomes a 3D network of isolated and/or connected space (Fig. 2.19), through which flow modelling can also be achieved (Talon et al. 2012).

2.2.4.1 Micro-CT Setup and 3D-Image Reconstruction

CT scan is commonly applied on a 23 mm core (plug) sample permitting the optimal selection of a representative miniplug of 5 mm diameter. This miniplug, which is micro-drilled in the core (plug) sample, will be subject to micro-CT scanning. Hence, 3D images could be acquired using a Nanotom high resolution X-ray micro-CT from PHOENIX X-Ray (e.g. De

Boever et al. 2012). The sample is fixed on a horizontal rotation axis, placed between the source and the detector. 2D projections are acquired by rotating the sample over 360° at rotation steps of 0.2° . Parameters during acquisition are a tube voltage of 90 kV and a current of $170 \mu\text{A}$. The detector consists of a Hamamatsu flat detector ($110 \text{ mm} \times 110 \text{ mm}$) made up of a 2304×2304 pixels (pxls) grid, with a step of $50 \mu\text{m}$. The source-object distance is 11.8 mm and the source-detector distance 200 mm, providing a resolution of $3 \mu\text{m}$ (pixel size). The presence of very fine pores and pore throats however required an even lower pixel size. To increase the resolution, the detector acquisition

Fig. 2.19 Extracted macro-pore network for the Estailades carbonate rock standard (France). The scale bar represents the width in microns of the pore space (courtesy of the IFPEN Petrophysics group)



mode is applied. By shifting the detector along the projection plan it creates a virtual detector of 2304×4608 pxls, allowing a larger field of view. Then the source-object distance is adjusted to 6.2 mm to double the magnification ratio. With this set up the resulting resolution is $1.5 \mu\text{m}$. In counterpart, the acquired data size and the acquisition time double. Further improved conditions may lead to higher resolutions, in the order of $0.5 \mu\text{m}$ —this certainly necessitates longer acquisition time.

Each acquisition (with a $1.5 \mu\text{m}$ resolution) generates 1800 TIFF projections that are used for the numerical reconstruction of volumetric data. The maximum volume that can be reconstructed and stored at full resolution is $1000 \times 1000 \times 1000$ pixels. The reconstruction (PHOENIX algorithm) uses a cone beam Feldkamp algorithm. The beam hardening effect is corrected by using a metal Cu-filter (0.1 mm) and by applying a mathematical correction during the reconstruction process.

2.2.4.2 Building an Equivalent Pore Network from the Actual Pore Space

The workflow for the image treatment and analysis of the reconstructed 3D-volumes consists of (1) visualizing, isolating (segmentation) and quantifying the resolved pore space and different mineral phases, (2) the reconstruction of an equivalent pore network and description of its parameters, and (3) the reconstruction of ancient pore networks.

The volume is visualized and analysed using the Avizo software package (version 6.2, VSG, France). In order to reduce noise, increase image contrast and facilitate thresholding, the image histograms are stretched and the images are filtered if appropriate (noise reduction, application of brightness/contrast filter). This results in an improved separation of the grey level peaks in the image histograms (Fig. 2.20). Segmentation of the grey level image to accurately separate each grey class one by one includes a

thresholding step, followed by filtering operations (removal of islands) and morphological operations (smoothing, shrinking and growing). More details can be found in Youssef et al. (2008). This creates a binary 3D image of each phase or grey class and allows calculating the volumetric percentages of the sample constituents. The quality of the image segmentation can be evaluated by comparing the calculated volumetric percentages with results of laboratory measurements on the 23 mm plug.

Porosity is compared to He-porosity measurements. Quantitative XRD results are used to calibrate the volumetric percentages for the different mineral constituents. The result of image segmentation is a 3D labelled binary image that allows visualizing the spatial distribution of each sample constituent. The pore space is typically composed of several, independent clusters. To further proceed, the pore space should include at least one, important percolating cluster to acquire representative results during transport property simulations.

Once a binary 3D image of the resolved pore space is captured, an equivalent network of pore bodies and pore throats can be built, which can be used in network models for the calculation of petrophysical properties. The procedure consists in three principal steps: skeleton extraction, pore space partitioning and parameter extraction (Fig. 2.21).

The skeleton extraction step uses the Distance Ordered Homotopic Thinning algorithm

implemented in Avizo. The algorithm computes the shortest distance of each point of the foreground (void space) to the background (solid phase). The resulting distance map is then used to guide the thinning algorithm, resulting in a thin, centralized skeleton that preserves the topography of the original pore space. By means of the distance map, each voxel of the skeleton is marked with the minimum distance to the boundary of the void space. The skeleton of the pore space is then partitioned into groups of lines belonging to the same pores and separated by throat points that correspond to the restrictions between pores. Subsequently, the different pores are geometrically separated and labelled by adding the binary image of the pore space to the labelled line set image using a voxel growth constrained algorithm. The process of pore network reconstruction allows defining several statistical parameters of the equivalent pore network, e.g. the pore size distribution, based on the pore radii and the coordination number of each pore (Youssef et al. 2008).

In addition, the ancient pore networks (shape, dimension, and inter-connectivity) could be reconstructed from 3D micro-CT images. Their transport properties may then be simulated (e.g. Talon et al. 2012). The procedure consists of an additional segmentation and pore network building step analogues to the procedure outlined above. The segmentation step involves a double thresholding operation. The present pore space is

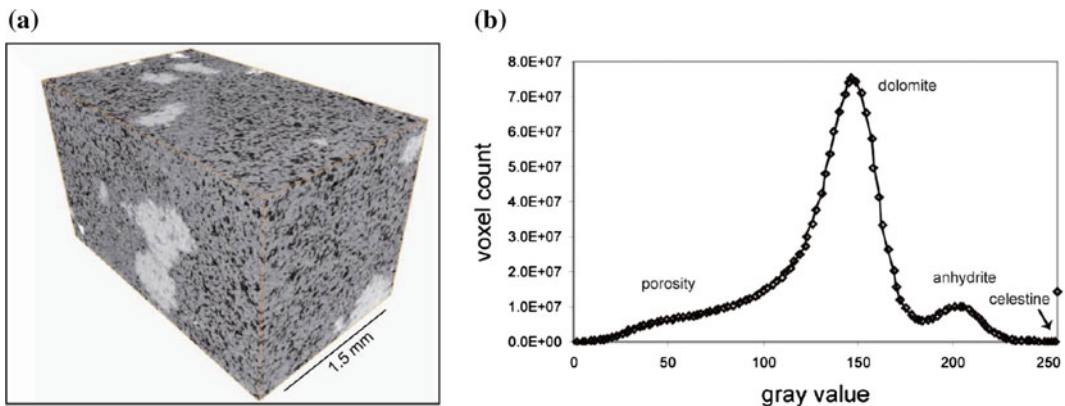


Fig. 2.20 **a** 3D grey scale view of micro-CT scan ($2000 \times 1000 \times 1000$ pxls) of a typical Jurassic Arab C dolostone (Middle East). **b** Grey level histogram (De Boever et al. 2012)

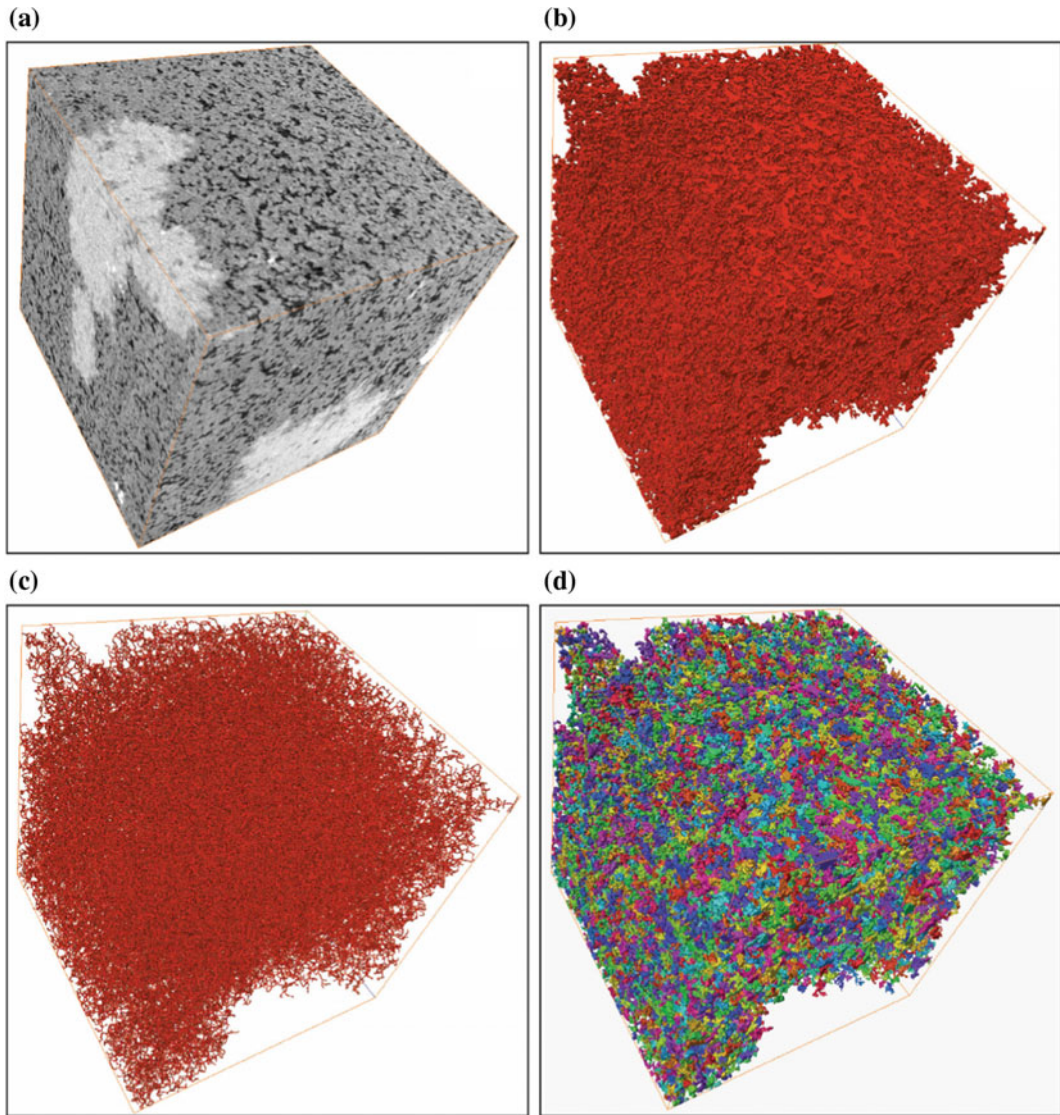


Fig. 2.21 Equivalent network building of the actual pore structure of a typical Jurassic Arab C dolostone (Middle East): **a** 3D grey scale view of micro-CT scan ($1000 \times 1000 \times 1000$ pxls); **b** Segmented image with

porosity in *red*, following the binarisation step; **c** 3D skeleton representation as *lines* in the *centre* of pores, preserving the original pore topography; **d** partitioned pore space of the entire volume

isolated and merged with the segmented volume of a second mineral phase. This approach has been applied on the typical (Jurassic) Arab C dolostones, whose intercrystalline porosity is plugged by anhydrite. The pore space before anhydrite precipitation (see Figs. 2.20 and 2.21), was accordingly reconstructed (for more details see De Boever et al. 2012).

2.2.4.3 Numerical Simulation of Mercury Intrusion and Permeability

Following pore space partitioning, a connection matrix is built that is used to simulate mercury intrusion and calculate the permeability. A full drainage curve is obtained through a step by step invasion of an entire pore volume that is

accessible via its throat radius for a fixed capillary pressure (P_c). The procedure is explained in detail by Youssef et al. (2007). Comparison of simulation results with lab permeability and Purcell mercury porosimetry measurements are used to validate the quality of the reconstructed pore network and pore partitioning (Fig. 2.22).

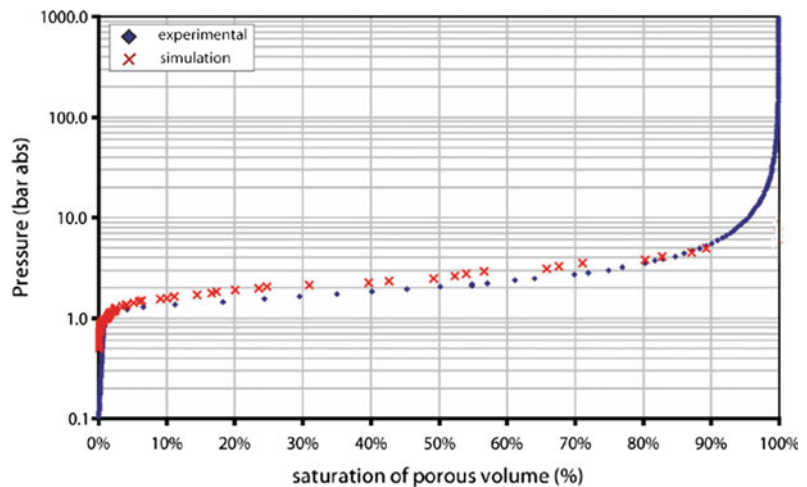
2.3 Discussion

Diagenetic processes can be unveiled through the detailed description of the related diagenetic phases. For example, petrographic examination of dolomite crystals together with geochemical and fluid inclusions analyses lead to suggest specific processes for their formation (i.e. conceptual models of dolomitization). In addition, dolomite studies have benefitted from exceptionally well exposed outcrops, where the geometry of the dolomitized geo-bodies could be apprehended (e.g. Shah et al. 2012; Dewit 2012). At Ranero (northern Spain), we have achieved relatively detailed mapping of such dolomite geo-bodies through analysis of aerial photographs and field observations (cf. Fig. 2.1). Still, petrography takes the largest share when conducting a typical study on diagenesis. Description and classification schemes of diagenetic phases (cements, replacive minerals, porosity) remain basically the outcome of

classical petrographic examinations whether with conventional, cathodoluminescence and/or scanning electron microscopic techniques.

A series of geochemical, mineralogical and fluid inclusion analyses are also carried out systematically within the framework of common diagenesis studies on carbonate rocks. Major and trace element compositions are frequently measured through geochemical analysis or electron microprobes. A variety of laboratory workflows (adapted to specific instruments: AAS, AES, LA-ICP-MS) are available, but I have chosen to highlight the ‘sequential extraction’ procedure that concerns samples containing both calcite and dolomite phases, in order to measure separately the major and trace elements of each phase (Nader 2003). Stable oxygen and carbon isotopic analyses are very common nowadays and they are carried out at specialized laboratories. Here, the ‘special double collection’ procedure that is applied on calcitized dolomites is presented (Nader et al. 2008). Though more expensive, strontium isotope analyses are also routinely carried out at specialized research centres, and the results of which illustrate most of the published work on diagenesis. XRD analysis is an old technique, yet today it benefits from Rietveld modelling, and results in a better assessment of the stoichiometry of dolomite crystals and quantified mineral volumes (further discussed in Chap. 3). New experimental protocols,

Fig. 2.22 Simulated and measured mercury injection capillary pressure curve of the actual pore structure of a typical Jurassic Arab C dolostone (Middle East)



developed at IFPEN are described in this chapter; they basically couple XRD and Rietveld refinement for studying dolomites. Microthermometry and crush-leach analyses involving fluid inclusions trapped in diagenetic minerals are also more or less frequently undertaken (especially the former method involving heating cooling stages mounted on microscopes). All of these techniques result in further characterizing the diagenetic phases and related diagenetic fluids, and the physico-chemical conditions prevailing at the time of their formation.

The optimal approach consists of integrating many—if not all—of these techniques. For example, oxygen isotopic ratios corresponding to specific cements are dependent on the original fluids from which they have precipitated and the prevailing temperatures. Combined with the measured liquid-vapour homogenization temperatures of relevant fluid inclusions trapped in these cements, the temperature at the time of precipitation can be constrained and therefore the original fluid oxygen isotopic ratio known (Friedman and O'Neil 1977; Land 1983; Fontana et al. 2010). Numerous papers illustrate well this approach (e.g. Nader et al. 2004, 2007, 2008; Fontana et al. 2014; among other published contributions). Besides, constraining the conditions of precipitation/formation of the diagenetic phases and their timing (for example with Sr isotopic ratios), together with petrographic examination lead to shaping up the paragenesis (check Fig. 2.11) and confirming the proposed conceptual model (Fig. 2.12). Ultimately, we are able to superpose the proposed sequence of diagenetic phases onto the burial curve (Fig. 2.23; Peyravi et al. 2014).

While recognizing that the field of 'diagenesis characterization' with its commonly used techniques is quite mature, some advancement and future perspectives appear to be very attractive. Measurements of 'Clumped' oxygen isotopes are becoming available for calcite and dolomite minerals (Dennis et al. 2011). This approach overcomes the dependence of classical oxygen isotopic ratios on both original fluids and temperatures (two variables, discussed above), providing estimations of the crystallization

temperatures based on the 'clumped' isotope standardized paleo-thermometry (check Figs. 2.13 and 2.14). Another interesting analytical technique involves magnesium isotopic analyses. Here, the source of Mg (major rock-forming element in terms of abundance) could be theoretically traced (Fig. 2.16). Today, this method is applied together with classical oxygen and strontium isotopic analyses and is proving to be of interest for constraining dolomitization processes (e.g. Lavoie et al. 2011). Better analytical precision with new techniques (LA-ICP-MS and TIMS) has provided successful applications of U-Pb dating on early and late diagenetic cements (Fig. 2.18). This is a powerful tool that will certainly become very attractive and will help in placing the various dated diagenetic phases on the burial curve (such as the one shown on Fig. 2.23). Through this approach, and together with other diagenetic information (deduced from stable and radiogenic isotopic and fluid inclusion analyses), the burial model can even be further calibrated (Mangenot et al. in press).

Characterizing diagenetic phases, and especially pore space, has been mostly achieved on 2D thin sections, leading in most of the cases to erroneous shapes and imprecise volumes. A significant future development involves the possibility to image—and characterize—the pore space in the three-dimensions by means of X-ray computed tomography (see further in Claes 2015). I have presented this method and related workflows based on the work of De Boever et al. (2012) on typical carbonate reservoir rocks. The details of CT and micro-CT approaches coupled with 3D-image analyses are tackled through describing the utilised setup, image reconstruction and segmentation, as well as building equivalent pore space networks (Fig. 2.21). This method overlaps with those discussed in the following chapter on 'quantitative diagenesis'. Qualitative characterization of pore space segmentation and inter-connectivity could still be done on micro-CT images. The more quantitative applications are discussed in Chap. 3.

CT and micro-CT techniques are very promising and will be further developed in the

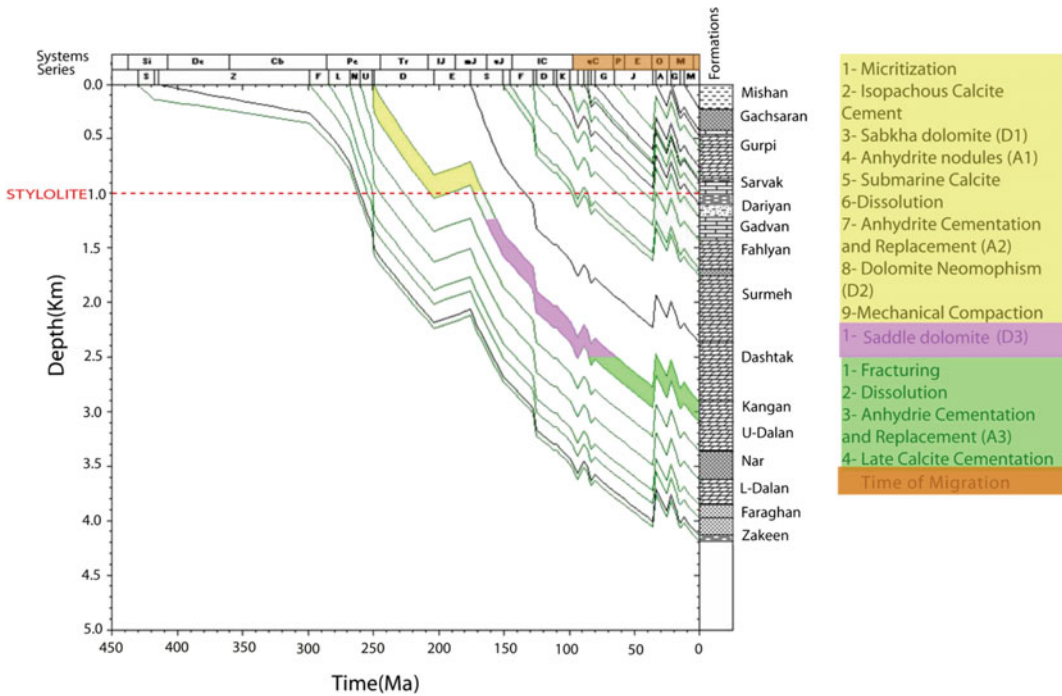


Fig. 2.23 Burial model for a well intercepting Khuff equivalent reservoirs (Kangan Formation) in the Salman field, offshore Iran. A simplified form of presenting the

various diagenetic phases superposed on the burial model is also illustrated (for more details refer to Peyravi et al. 2014)

near future for capturing the pore space in 3D (applied for instance through EOR research projects). Scanning resolution needs to be enhanced to capture micro-porosity within grains. In addition, improved intensity separation is needed to be able to better distinguish diagenetic phases. We have also argued the importance of integrating such approach with SEM, microprobe and XRD techniques (De Boever et al. 2012). The eventual perspective of 3D pore space characterization is to come up with new porosity classification schemes taking into account the real dimensions and connectivity of pores.

The new generation of porosity assessment methods (and possible diagenetic minerals volumetric determination) is believed to be associated to the micro-CT technique coupled with computer-based image analysis. Still, an important challenge is associated to defining the representative elementary volume, which has been introduced in Chap. 1 and will be further

discussed in the following chapter dedicated to methods of quantitative diagenesis. How to characterize vuggy porosity, if the vugs are larger than the sample under investigation? And what methods to follow to make sure that the analysed sample can represent the reservoir rock? Besides, thin sections and sample-plugs do not take into account fracture porosity, which is known to have crucial impact on carbonate reservoirs. This is commonly addressed, while constructing reservoir models, by making use of oil/gas fields production tests and geophysical-based extrapolations, failing to capture the finer-scale of lithofacies and diagenesis distributions. Alternatively, ‘upscaling’ in reservoir modelling remains very challenging. In many cases, it reverts to simplified average values representing mixed lithofacies of contrasting reservoir properties. REVS and ‘upscaling’ are two research subjects form important scientific challenges for achieving multi-scale numerical models of diagenesis.

2.4 Advancement in Characterization of Diagenesis

Several approaches and methods are becoming very attractive for improving our capability of characterizing carbonate reservoir rocks at various scales. Diagenetic processes with their impacts on rock properties need to be further understood. The diagenetic phases (outcome of diagenetic processes) can be precisely described by means of a variety of methods. The most commonly used methods combine petrographic, geochemical and fluid inclusion analyses. They result in characterizing the diagenetic phases and the prevailing physico-chemical conditions at the time of their formation. Thus, available analytical methods—and enhanced techniques—not only lead to better diagenesis characterization but they also unravel the mechanisms of related processes, and eventually their impacts on reservoir properties.

Field observations (and/or well cores investigations) are the starting point of any diagenesis research project. Therefore, improved field (well cores) data-collection, whereby considerable investigation/observation is made at outcrop (and/or on well cores) should be achieved. Based on my experience, there should be a trend towards decreasing the number of samples (and material), while increasing their representative significance. In addition, defining the Representative Elementary Volumes (REVs) needs to be attempted for each study.

One of the future developments that will also improve the efficiency and precision of diagenesis characterization is related to computer-

assisted petrographic analyses (on conventional microscopic techniques as well as SEM-EDS, EMPA) and image analyses. The key targets will be to undertake faster, and more systematic characterization (of sedimentological and diagenetic features—including porosity).

New analytical techniques for geochemical and mineralogical assessment of the host rocks as well as diagenetic phases are still needed. EMPA is a powerful tool to characterize the distribution of mineralogical variability in carbonate rocks. Mg- and clumped-oxygen isotopic analyses start to be applied to constrain the nature of diagenetic fluids and temperatures of precipitation of diagenetic phases, respectively. U-Pb method has proved to be suitable for dating diagenetic phases. Clumped-oxygen isotope analyses coupled with U-Pb dating provide not only more precise characterization of diagenetic phases, but also suitable proxies for burial history calibration. This will be very much needed for adequately overlaying the diagenetic stages on burial models and for adjusting associated numerical simulations.

Three-dimensional scanning of cores and samples (via computed tomography) is certainly expected to achieve better performance and higher resolutions (e.g. capturing cement phases). Porosity description and classification has always been associated to the host rock textures. Today's technology allows the characterization of the pore space directly, and in 3D (e.g. micro-CT). This will lead inevitably to a new, innovative approach to describing and classifying the pore space in reservoir rocks. The new classification scheme should have a better connection with related permeability.



<http://www.springer.com/978-3-319-46444-2>

Multi-scale Quantitative Diagenesis and Impacts on
Heterogeneity of Carbonate Reservoir Rocks

Nader, F.H.

2017, XXXVI, 146 p. 107 illus., 92 illus. in color.,

Hardcover

ISBN: 978-3-319-46444-2